Extraordinary infrared transmission through a periodic bowtie aperture array

Edward C. Kinzel and Xianfan Xu*

School of Mechanical Engineering and Birck Nanotechnology Center, Purdue University, West Lafayette, Indiana 47907, USA
**Corresponding author: xxu@purdue.edu*

Received December 14, 2009; revised February 19, 2010; accepted February 22, 2010; posted March 3, 2010 (Doc. ID 121434); published March 26, 2010

The discovery of extraordinary transmission through periodic aperture arrays has generated significant interest. Most studies have used circular apertures and attributed enhanced transmission to surface plasmon polariton (SPP) resonances and/or Rayleigh–Wood anomalies (RWA). Bowtie apertures concentrate light and have much longer cutoff wavelengths than circular apertures and can be designed to be strongly resonant. We demonstrate here that the total transmission through a bowtie aperture array can exceed 85% (4× the open area). Furthermore, we show that the high transmission is due to waveguide modes as opposed to the commonly believed SPP/RW phenomena. This work is focused on IR wavelengths near 9 μm; however, the results are broadly applicable and can be extended to optical frequencies. © 2010 Optical Society of America

OCIS codes: 240.0240, 240.6680, 050.1220.

Classical aperture theory predicts that transmission through a subwavelength hole scales with $(d/\lambda)^4$, where d is the diameter of the aperture and λ is the free-space wavelength of light [1,2]. The discovery of the extraordinary transmission through subwavelength hole arrays has generated significant interest [3–5]. However, debate still exists as to the exact physical mechanism behind the enhancement [6]. A number of studies have shown that the transmission enhancement occurs near the Bragg condition of the propagating surface plasmon polaritons (SPPs) [7,8]. This occurs for conditions similar to the Rayleigh–Wood anomaly (RWA), which happens when higher diffraction orders are directed along the surface [9]. In either case, energy is trapped at the surface and, once trapped, tunnels through the hole array before being scattered. In addition to propagating SPP modes, localized surface plasmon resonances also have been shown to play a role [10]. It has also been noted that the cutoff wavelength is considerably longer for a waveguide defined in a real metal than in PEC due to hybridization with SPP modes in the holes [11,12]. If the apertures are not symmetric, the transmission becomes polarization dependent [5,13]. 90% transmission has been achieved through annular aperture arrays [14,15]. Larger, open apertures such as circles [16,17], rectangles [16], and crossed dipoles [17] have also been investigated, showing the influence of both aperture shape and surface resonances in the mid- and long-IR wavelengths.

In this Letter we investigate transmission through a periodic array of bowtie apertures. The transmission modes are optimized to obtain high transmission around $\lambda = 9$ μm. The high transmission in IR has the potential as a high-efficiency IR coupler for detection devices. The bowtie aperture is also polarization selective, therefore useful where polarization selectivity is of interest such as IR polarimetry imaging [18]. The fundamental principles in IR are similar to those in visible wavelengths, and therefore the bowtie aperture arrays studied in this work are scalable to visible wavelengths.

Bowtie apertures are one type of ridge aperture [2,19–22]. A key advantage of the ridge aperture is that the cutoff wavelength is much longer than that in the circular or rectangular aperture while providing electric field confinement. Ridge apertures can also be designed to provide strong resonant effects that permit enhanced transmission even for an isolated aperture [21,22]. Field concentration and enhancement in bowtie apertures have been experimentally demonstrated (in visible wavelengths), including near-field scanning microscopy (NSOM) measurements [23] and nanolithography [24].

The geometry of the bowtie aperture array studied in this work is shown in Fig. 1, with periodicity p_x and p_y. The aperture profile described by Fig. 1 is selected to capture the profile produced by FIB milling. The geometry is defined by outline dimensions a and b with a gap defined by d, and the apertures are milled in a free-standing gold film with thickness $t = 1.25$ μm. The array presented in this study is characterized by $a = 3.20$ μm, $b = 1.80$ μm, $p_x = 4.35$ μm, $p_y = 2.85$ μm, $d = 0.11$ μm, $\theta = 2.5°$, $r_1 = 4.00$ μm, $r_2 = 0.25$ μm, $r_3 = 0.13$ μm, and $r_4 = 0.05$ μm. These dimensions are determined by fitting scanning electron

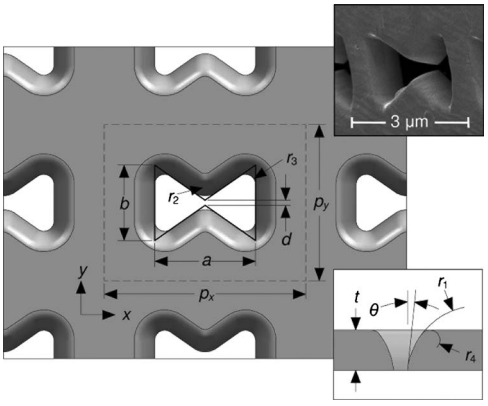

Fig. 1. Simulated geometry of focused-ion-beam (FIB) milled bowtie aperture array (not drawn to scale). Insets, an SEM image taken at 52° and a cross-section on the yz plane through the gap of one of the apertures.

microscopy images of the apertures designed to maximize transmission near $\lambda = 9\ \mu$m.

A $170 \times 160\ \mu$m array (40×56 apertures) was milled using an FEI Nova 200 dual-beam FIB (30 kV, 3 nA Ga+ beam current). Transmission through the array was measured with a Bruker Vector 22 FTIR with an IRScope I and is plotted in Fig. 2. The polarization of the light was selected by placing a holographic wire-grid linear polarizer in the optical path. The maximum transmission of y-polarized light through the array is measured to be 85% and occurs at the wavelength of 9.4 μm. If the transmission is normalized to the open area of the arrays, the maximum transmission is ~400%. The measured polarization extinction ratio between the y- and x-polarized light is greater than 300 for $8.5\ \mu\text{m} < \lambda < 12.5\ \mu$m.

Numerical studies using a frequency-domain finite-element method solver [25] were performed to design and optimize the aperture arrays prior to fabrication. Periodic boundary conditions were employed to simulate an infinite array except for the isolated aperture case, where absorbing boundaries were used. The permittivity of gold is taken from [26]. We start by calculating the transmission through an isolated aperture, which is determined by integrating the Poynting vector over the exit plane of the aperture and normalizing it to the intensity on the open area. Figure 3(a) shows that at resonance the light diffracted from the aperture exceeds the light incident on its open area by a factor of 3 for y-polarized light. The peak at $\lambda = 4\ \mu$m corresponds to the first Fabry–Perot resonance of the TE_{10} waveguide mode.

Figures 3(b) and 3(c) show the field structure extracted from the lowest-order eigenmode simulation of an isolated aperture. This mode occurs at $\lambda = 10.4\ \mu$m and corresponds to the cutoff condition for the TE_{10} waveguide mode. At cutoff, the propagation constant approaches zero and the magnetic field within the aperture is almost completely directed in the z direction. As shown in Figs. 3(b) and 3(c), the electric field is well confined in the gap while the magnetic field forms inductive loops circulating through the open arms of the aperture. These fields are almost completely polarized in the yz and xz planes, respectively, which makes the coupling to the resonant mode very polarization dependent. Because the electric field is confined to the gap region (much smaller than the free-space wavelength), the aperture radiates similar to a Hertzian dipole.

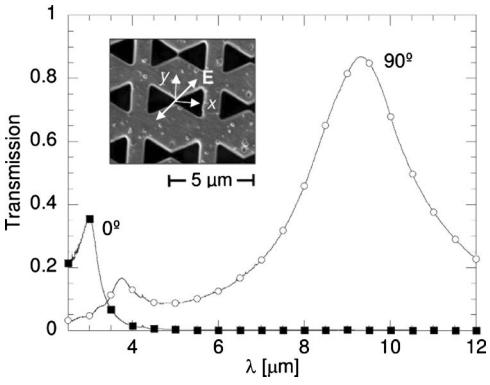

Fig. 2. Experimental results for the normally illuminated bowtie aperture array at 0° and 90° polarizations. The inset is an SEM image of the array.

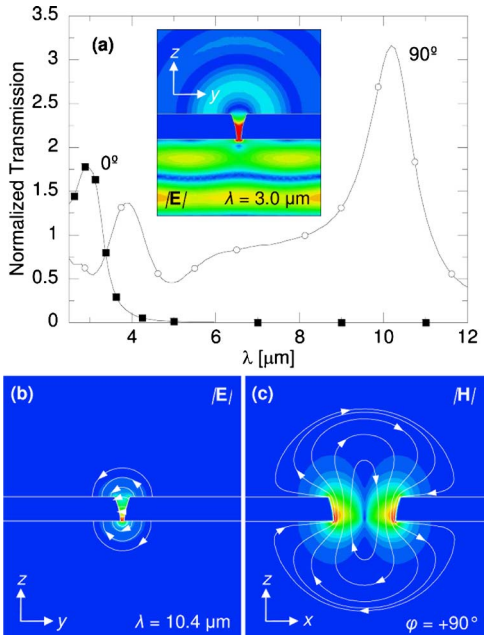

Fig. 3. (Color online) Simulated response from an isolated aperture: (a) transmission spectra, field distributions from eigenmode simulation; (b) electric field in the yz plane and (c) magnetic field in the xz plane.

When apertures are assembled to form an array, they constructively interfere to provide the T_{00} diffraction order under normal incidence (this is the only diffraction order for $\lambda > p_x$). Figure 4 shows the simulated transmission through an infinite array of apertures. The numerical results are in good agreement with the experimental results (Fig. 2). Figure

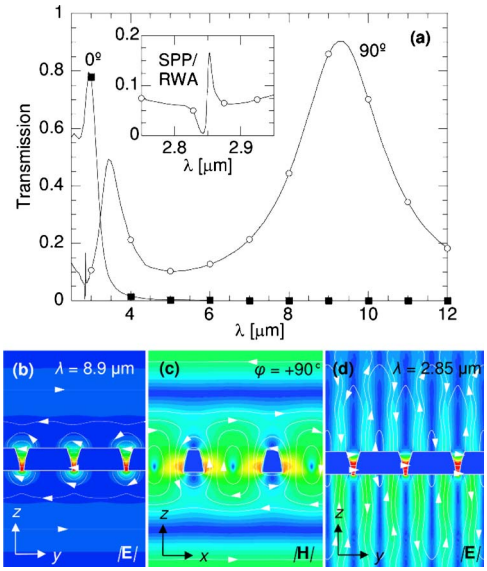

Fig. 4. (Color online) Simulation results of an array of bowtie apertures: (a) transmission spectra with close-up of SPP/RWA in inset, (b) electric field in the yz plane (c) magnetic field in the xz plane, both for the TE10 mode, and (d) electric field on the yz plane for the SPP/RWA.

4(a) also shows the Fabry–Perot peak at about 4 μm, which was also seen in the experimental data and in the simulation result of a single bowtie aperture [Fig. 3(a)]. The resonant peak is blueshifted from the case of the isolated aperture. This is due to inductive coupling between adjacent apertures. Figures 4(b) and 4(c) show the electric and magnetic field structures for this resonance extracted from an eigenmode simulation. As was the case for the isolated aperture, the electric field remains well confined in the gap region in each aperture. The magnetic field is aligned with the z direction within the aperture, indicating a TE_{10} mode, and circulates between adjacent apertures, further reducing its confinement. This magnetic coupling greatly increases the effective area of the aperture, permitting more incident radiation to transmit through the array. The spacing between the apertures is critical to maximize this effect.

The isotropic nature of the transmission from an isolated aperture suggests the possibility of grating phenomena when λ or $\lambda_{SPP}=p_y$ (in the IR, $\lambda_{SPP}\approx\lambda$, since the imaginary part of the permittivity of metal is sufficiently large). The simulation results do show a weak RWA/SPP feature at $\lambda=2.85$ μm [inset of Fig. 4(a)]. Figure 4(d) shows the field distribution corresponding to this mode. The magnitude of the RWA/SPP is small compared with the waveguide mode at 9.4 μm. This is further exacerbated by the roughness of the film, which serves to scatter the surface mode, making it difficult to detect in the experiment.

In summary, this work demonstrates extraordinary IR transmission through a bowtie aperture array. The high transmission is shown to be the result of coupling to and from resonant waveguide modes for both a bowtie array and a single bowtie aperture with surface-mode phenomena playing a negligible role. The mode structures of the apertures are shown to be inductively coupled to each other when the apertures are placed in the array, which contribute to the extraordinary transmission of the aperture array.

Support to this work by the Air Force Office of Scientific Research STTR program (contract FA9550-09-C-0058, Program Manager Dr. Gernot Pomrenke), National Science Foundation (NSF) (DMI-0707817), and Defense Advanced Research Projects Agency (DARPA) (grant N66001-08-1-2037, Program Manager Dr. Thomas Kenny) is gratefully acknowledged. The authors also thank John Coy of the Purdue University Birck Nanotechnology Center for assistance in taking the FTIR measurements and Dr. Axel Reisinger of QmagiQ LCC and Prof. W. J. Chappell of Purdue University for helpful discussions.

References

1. H. A. Bethe, Phys. Rev. **66**, 163 (1944).
2. D. M. Pozer, *Microwave Engineering* (Wiley, 2003).
3. C. Genet and T. W. Ebbesen, Nature **445**, 39 (2007).
4. T. W. Ebbesen, H. J. Lezec, H. F. Ghaemi, T. Thio, and P. A. Wolff, Nature **391**, 667 (1998).
5. R. Gordon, A. G. Brolo, A. McKinnon, A. Rajora, B. Leathem, and K. L. Kavanagh, Phys. Rev. Lett. **92**, 037401 (2004).
6. H. Leznec and T. Thio, Opt. Express **12**, 3629 (2004).
7. L. Martín-Moreno, F. J. García-Vidal, H. J. Lezec, K. M. Pellerin, T. Thio, J. B. Pendry, and T. W. Ebbesen, Phys. Rev. Lett. **86**, 1114 (2001).
8. F. J. Garcia de Abajo, Rev. Mod. Phys. **79**, 1267 (2007).
9. H. Gao, J. M. McMahon, M. H. Lee, J. Henzie, S. K. Gray, G. C. Schatz, and T. W. Odom, Opt. Express **17**, 2334 (2009).
10. S. Wu, Q. Wan, X. Yin, J. Li, D. Zhu, S. Liu, and Y. Zhu, Appl. Phys. Lett. **93**, 101113 (2008).
11. R. Gordon and A. G. Brolo, Opt. Express **13**, 1933 (2005).
12. P. B. Catrysse, H. Shin, and S. Fan, Vac. Sci. Technol. **23**, 2675 (2005).
13. K. J. Klein Koerkamp, S. Enoch, F. B. Sagerink, N. F. van Hulst, and L. Kuipers, Phys. Rev. Lett. **92**, 183901 (2004).
14. W. Fan, S. Zhang, B. Minhas, K. J. Mallor, and S. R. J. Brueck, Phys. Rev. Lett. **94**, 033902 (2005).
15. Y. Poujet, J. Salvi, and F. I. Baida, Opt. Lett. **32**, 2942 (2007).
16. Y. H. Ye, Y. Cao, Z. B. Wang, D. Yan, and J. Y. Zhang, Appl. Phys. Lett. **94**, 081118 (2009).
17. Y. Ye, Z. Wang, D. Yan, and J. Zhang, Opt. Lett. **32**, 3140 (2007).
18. G. P. Nordin, J. T. Meier, P. C. Deguzman, and M. W. Jones, J. Opt. Soc. Am. A **16**, 1168 (1999).
19. J. Helszajn, *Ridge Waveguides and Passive Microwave Components* (Institution of Electrical Engineers, 2000).
20. R. D. Grober, R. J. Schoelkoph, and D. E. Prober, Appl. Phys. Lett. **70**, 1354 (1997).
21. K. Şendur, W. Challener, and C. Peng, J. Appl. Phys. **96**, 2743 (2004).
22. E. X. Jin and X. Xu, Jpn. J. Appl. Phys. **43**, 407 (2004).
23. L. Wang and X. Xu, Appl. Phys. Lett. **90**, 261105 (2007).
24. L. Wang, S. M. Uppuluri, E. X. Jin, and X. Xu, Nano Lett. **6**, 361 (2006).
25. HFSS 12.0, Ansoft LLC (2009).
26. M. A. Ordal, L. L. Long, R. J. Bell, S. E. Bell, R. W. Alexander, Jr., and C. A. Ward, Appl. Opt. **22**, 1099 (1983).